Identification of potential miR-155 target genes in epidermal immune microenvironment of atopic dermatitis patients and their inflammatory effects on HaCaT cells

XIAOCHEN WANG[1*], LU CHEN[1*], XIAOQING CHEN[1*], CHANG LIU[1], WENHONG QIU[1] and KAIWEN GUO[2]

[1]Department of Immunology, School of Medicine, Jianghan University, Wuhan, Hubei 430056; [2]Department of Pathogenic Biology, Medical College, Wuhan University of Science and Technology, Wuhan, Hubei 430065, P.R. China

Abstract. Atopic dermatitis (AD) is a common inflammatory skin condition and the leading cause of morbidity associated with skin conditions worldwide. For the majority of patients, AD is a lifelong disease that cannot be cured completely. Therefore, in the present study, differentially expressed genes (DEGs) in the epidermal immune microenvironment were screened using bioinformatic techniques. Subsequently, an *in vitro* cellular model was constructed to investigate the role of microRNA (miR)-155 in immune infiltration during AD. In the present study, two datasets (GSE121212 and GSE157194) were downloaded from Gene Expression Omnibus, before the DEGs were screened and subjected to Gene Ontology and Kyoto Encyclopedia of Genes and Genomes functional enrichment analyses. miRNet was used to predict the possible target genes of miR-155 among the differentially expressed genes found. Consequently, peptidase inhibitor 3 (PI3), FOS-like 1, AP-1 transcription factor subunit (FOSL1), C-X-C motif chemokine ligand (CXCL)1 and CXCL8 were selected to be the potential target genes of miR-155 in the epidermal immune microenvironment of patients with AD. Concurrently, an inflammatory cell model using HaCaT cells was constructed by TNF-α and IFN-γ treatment. The effects of miR-155 on HaCaT cell proliferation and secretion of IL-1β, IL-6, IL-10, IL-15, PI3, FOSL1, CXCL1 and CXCL8 under inflammatory and non-inflammatory conditions were then analyzed. The results showed that after the HaCaT cells were transfected with miR-155, miR-155 inhibited HaCaT cell proliferation and decreased the mRNA expression levels of PI3 and CXCL8, increased the mRNA levels of FOSL1 and secretion levels of IL-1β, IL-6, IL-15 and CXCL1. By contrast, miR-155 decreased the secretion levels of IL-10 and CXCL8. In the inflammatory cell model of HaCaT cells, miR-155 was found to significantly inhibit the proliferation of HaCaT cells during inflammation whilst significantly increasing the secretion of IL-1β, IL-6, IL-10 and IL-15. In addition, miR-155 increased the mRNA expression and secretion levels of CXCL1 and CXCL8, whilst also increasing the mRNA expression levels of PI3. Results from the current study suggest that miR-155 can stimulate keratinocytes to produce inflammatory cytokines and proteins to enhance the inflammatory response in AD.

Introduction

Atopic dermatitis (AD) is a common chronic inflammatory skin disease that is characterized by eczema-like lesions accompanied by intense itching. This condition affects individuals of all age groups and ethnicities, with 20% children and 10% adults suffering from this condition in high-income countries. Although this condition is typically non-fatal, it does place significant burden on the patient (1,2). The pathogenesis of AD involves a multitude of factors, including skin barrier disorders, microbial dysbiosis and immune dysregulation. These factors interact in a complex multidirectional network that can exacerbate atopic skin diseases, although targeted therapies can also alleviate the condition (3). Combating skin barrier dysfunction has been an important aspect of clinical management for this disease, with topical emollients being the first-line treatment for AD (4).

The skin provides a key physical barrier between the body and the external environment. This barrier structure consists of the cuticle and tight junctions, which prevents transepithelial water loss and the entry of external antigens (5). Damage to skin barrier function leads to increased sensitivity of the body to environmental allergens and various stimuli, triggering an inflammatory cascade reaction, leading to immune disorders

---

Correspondence to: Dr Wenhong Qiu, Department of Immunology, School of Medicine, Jianghan University, 8 Sanjiaohu Road, Caidian, Wuhan, Hubei 430056, P.R. China
E-mail: qiuwenhong@jhun.edu.cn

Dr Kaiwen Guo, Department of Pathogenic Biology, Medical College, Wuhan University of Science and Technology, 2 Huangjiahu West Road, Hongshan, Wuhan, Hubei 430065, P.R. China
E-mail: guowendy@wust.edu.cn

*Contributed equally

and eventually the onset of AD. However, the specific mechanism underlying this process remains unclear.

Skin lesions as a result of AD have been observed to exhibit the dysregulated expression of several genes associated with keratinocyte activity and T cell infiltration, including Th2-related genes (such as IL-4, IL-10 and IL-13) and Th22-related genes (such as IL-22) (6,7). In addition, cytokines serve an important role in mediating inflammatory responses and regulating the immune response. Transcriptomic sequencing is becoming increasingly popular in recent years for analyzing the mechanism underlying the roles mediated by differentially expressed genes (DEGs) in AD and improving understanding into this disease.

MicroRNAs (miR/miRNA) can participate in various regulatory processes, such as virus defense, cell proliferation, cell apoptosis and organ formation, in addition to serving an important role in regulating the inflammatory response in a number of diseases, including AD (8).

miR-155 serves an important role in the pathogenesis of AD. miR-155 is expressed by cutaneous T cells, dendritic cells and mast cells. Previously studies have shown that miR-155 is overexpressed in patients with AD, such that it is the most significantly upregulated microRNA in terms of expressions (9,10). It can enhance T cell proliferation by inhibiting cytotoxic T lymphocyte associated antigen-4 (CTLA-4) (11). In AD mouse models, miR-155 has been shown to target cAMP-dependent protein kinase inhibitor α and regulate tight junction protein expression, which in turn affect epithelial barrier function (10). In the skin model of AD, IL-32 has been reported to promote the expression of Janus kinase 1 and upregulate miR-155 expression, leading to the occurrence of AD inflammation (9). Although evidence on the role of miR-155 in the pathogenesis of AD has been accumulating, the mechanism of miR-155 underlying the development of AD remains unclear and requires further research.

To investigate the role of miR-155 in the pathogenesis of AD, a human immortalized keratinocyte cell line HaCaT was used as an *in vitro* model to screen for DEGs in the epidermal immune microenvironment. In addition, immune cell infiltration and prediction miR-155 target genes were assessed using bioinformatic techniques. The aim of the present study was to investigate the mechanism of miR-155 in immune infiltration in AD and provide novel gene targets for diagnosis and treatment.

Materials and methods

Data acquisition and processing. The gene expression profile datasets were retrieved from the GEO database (https://www.ncbi.nlm.nih.gov/gds/) according to the following conditions: i) For AD; ii) the biological type was human; and iii) the sample type was skin tissue. Finally, GSE121212 (12) and GSE157194 (13) were selected as the subject of research and analysis. GSE121212 included skin biopsy specimens from lesion and non-lesion sites from 21 patients. By contrast, GSE157194 included lesion skin samples from 57 patients and non-lesion skin samples from 54 of these patients. The gene expression matrices of GSE121212 and GSE157194 were downloaded from the GEO database.

Screening for DEGs. DEGs were screened using the R-package (R version 4.2.3; http://www.R-project.org/) 'limma-voom'

(version 3.40.6) (14) and the screening criteria were as follows: log fold change >2, P<0.05. Fold change is the fold change of the DEGs. The DEGs after screening were visualized in the form of a heat map and a volcano map.

Screening for differentially co-expressed genes in the two datasets. The DEGs found in GSE121212 and GSE157194 were cut from the VENNY 2.1.0 website (https://bioinfogp.cnb.csic.es/tools/venny/) to obtain the differentially co-expressed genes.

Gene Ontology (GO) functional enrichment and Kyoto Encyclopedia of Genes and Genomes (KEGG) pathway enrichment analysis of differentially co-expressed genes. The R software package 'Cluster Profiler' (version 4.8.3, https://bioconductor.org/packages/release/bioc/html/clusterProfiler.html) was used to perform GO function enrichment and KEGG pathway enrichment analysis of differentially co-expressed genes, before the enrichment results of differentially co-expressed genes were obtained. P<0.05 was used as the evaluation standard and visual analysis was performed. The GO analysis included the following three aspects: Biological process (BP), molecular function (MF) and cellular localization (CC).

Prediction of target genes of miR-155-3p. The downstream target genes of miR-155-3p were predicted using the miRNet 2.0 website (https://www.mirnet.ca/miRNet/home.xhtml). VENNY 2.1.0 site was used to screen for the intersection of the significantly different co-expressed genes and the downstream target genes of miR-155-3p, using which the genes designated for further studies would be screened.

Construction of the protein-protein interaction (PPI) network. As proteins rarely function alone, there was a need to study the interactions among proteins. To identify potentially important protein interactions, significantly differentially co-expressing genes were screened using the adjusted log fold change >2, P<0.05. The selected significantly differentially coexpressing genes were imported into the STRING 12.0 database (https://cn.string-db.org/) to construct a PPI network.

Searching the gene expression data in HaCaT cells. The Human Protein Atlas website (https://www.proteinatlas.org/) provides the RNA expression data (normalized transcript per million values of cell lines) of different genes in different cell lines; therefore, The Human Protein Atlas was used to identify the expression levels of target genes in HaCaT cells.

Cell culture and inflammatory cell model. HaCaT cells (cat. no. CL-0090; Procell Life Science & Technology Co., Ltd.) were cultured in minimal essential medium (Procell Life Science & Technology Co., Ltd.) supplemented with 10% FBS (Procell Life Science & Technology Co., Ltd.) at 37˚C in 5% CO_2. The cells were treated with or without TNF-α and IFN-γ (5 ng/ml; PeproTech, Inc.) for 6 h. At this time, the cells were termed the 'TI' group.

Transfection with the miR-155 mimics or inhibitor. HaCaT cells were first seeded into six-well plates at a density of $1x10^7$ cells/ml. At 80% confluence, the cells were treated with 100 pmol either miR-155 inhibitor (5'-AACCCCUAU

CACGAUUAGCAUUAA-3') or the inhibitor control (5'-GUC CCUCACAUCAUAAGCUAAUAA-3'), or with miR-155 mimics (sense, 5'-UUAAUGCUAAUCGUGAUAGGG GUU-3' and antisense, 5'-CCCUAUCACGAUUAGCAUUA AUU-3') or with the mimics control (sense, 5'-UUCUCC GAACGUGUCACGUTT-3' and antisense, 5'-ACGUGACAC GUUCGGAGAATT-3') (Shanghai GenePharma Co., Ltd.) using Lipofectamine® 2000 (Thermo Fisher Scientific, Inc.), according to the manufacturer's protocols. The RNA-lipid complexes were first added to the HaCaT cells before the medium was changed after 6 h, and the cells continued to be transfected at 37°C for 42 h.

Reverse transcription-quantitative PCR (RT-qPCR). Different groups of HaCaT cells were lysed with 1 ml TRIzol® reagent (Thermo Fisher Scientific, Inc.) for 5 min. Then, 200 μl chloroform was added to the lysed samples for 3 min at room temperature. Following centrifugation at 13,400 x g for 15 min at 4°C, the supernatant was collected and mixed with 500 μl isopropanol. The mixture was then kept at 4°C for 10 min. The sample was removed and centrifuged at 13,400 x g for 15 min at 4°C. The supernatant was discarded and the pellet was washed twice with 500 μl 75% ethanol (centrifuged at 13,400 x g for 5 min at 4°C). Total RNA was obtained by adding 20 μl RNase-free ddH$_2$O. cDNA was synthesized with ReverTra Ace® qPCR RT Kit (Toyobo Life Science), according to the manufacturer's protocol. Gene expression levels were determined in the CFX Connect Real-Time System (Bio-Rad Laboratories, Inc.) using the SYBR Green PCR Master Mix (Thermo Fisher Scientific, Inc.). The miR-155-5p and U6 specific bulge loop miRNA RT-qPCR primer sets (one RT primer and one pair of qPCR primers in each set) were developed by Sangon Biotech Co., Ltd. GAPDH was used as an internal control for mRNA normalization and U6 was used as an internal control for miRNA normalization. The thermocycling conditions were as follows: Initial denaturation at 95°C for 30 sec; followed by 40 cycles of denaturation at 95°C for 5 sec, and annealing and elongation at 60°C for 30 sec. The mRNA primer sequences used for RT-qPCR (Sangon Biotech Co., Ltd.) were as follows Human Elafin forward, 5'-CACTGT CAAAGGCCGTGTTC-3' and reverse, 5'-GCGGTTAGG GGGATTCAACAG-3'; human FOS-like 1, AP-1 transcription factor subunit (FRA1 or FOSL) forward, 5'-CTGACC TACCCTCAGTACAGC-3' and reverse, 5'-AAGTCGGTC AGTTCCTTCCTC-3'; human C-X-C motif chemokine ligand (CXCL)1 forward, 5'-GGGAATTCACCCCAAGAACAT C-3' and reverse, 5'-GGATGCAGGATTGAGGCAAGC-3'; human CXCL-8 forward, 5'-CACTGCGCCAACACAGAA AT-3' and reverse, 5'-GCCCTCTTCAAAAACTTCTCC AC-3' and human GAPDH forward, 5'-AATTCCATGGCA CCGTCAAG-3' and reverse, 5'-AGCATCGCCCCACTTGAT TT-3'. Gene expression was normalized to that of GAPDH or U6 expression and relative expression was calculated using the $2^{-\Delta\Delta Cq}$ method (15).

Measurement of cell proliferation. HaCaT cells were seeded into 96-well plates at a density of 1.5x10^4 cells/well. Cell Count Kit-8 (CCK8; Dojindo Laboratories, Inc.) reagent was added at 90% confluence of the cells according to the manufacturer's protocols. After incubation at 37°C for 2 h, the absorbance

value of each well was measured at wavelength of 450 nm using a microplate reader.

Measurement of cytokine levels. The concentrations of IL-1β (cat. no. E-EL-H0149c), IL-6 (cat. no. E-EL-H6156), IL-10 (cat. no. E-EL-H6154), IL-15 (cat. no. E-EL-H0222c), CXCL1 (cat. no. E-EL-H0045c) and CXCL8 (cat. no. E-EL-H6008) in cell culture supernatants were measured using ELISA kits (Elabscience Biotechnology, Inc.) according to the manufacturer's protocols.

Western blotting analysis. The cells were scraped following the addition of the RIPA protein lysis solution (RIPA: phenyl-methylsulfonyl fluoride, 100:1). Samples were then collected into microcentrifuge tubes and lysed for 20 min. The protein concentrations of the samples were determined with a BCA protein assay kit (Beyotime, Institute of Biotechnology). Total protein extracts (25 μg) were separated by SDS-PAGE on 10% gels and transferred to PVDF membranes. The membranes were blocked with a Blocking Buffer (Beyotime Institute of Biotechnology) for 1.5 h at room temperature and washed three times for 15 min each with TBS -0.1% Tween at room temperature. The membranes were then incubated overnight at 4°C with antibodies directed against Elafin (cat. no. ab184972; 1:1,000 dilution; Abcam), FRA1 (cat. no. 5281; 1:1,000 dilution; Cell Signaling Technology, Inc.) or β-tubulin (cat. no. 10094-1-AP; 1:200,000 dilution; ProteinTech, Inc.). After the membranes were washed, they were probed with a HRP-linked goat anti-rabbit IgG antibody (cat. no. A0208; 1:1,000 dilution; Beyotime Institute of Biotechnology) or the HRP-linked goat anti-mouse IgG antibody (cat. no. A0216; 1:1,000 dilution; Beyotime Institute of Biotechnology) for 1 h at room temperature. Protein bands were detected with the Immobilon Western Chemiluminescent HRP Substrate (cat. no. P0018S, Beyotime Institute of Biotechnology) and protein expression was quantified with a gel analysis software. The density of each specific band was measured using ImageJ software V1.53t (National Institutes of Health).

Statistical analysis. Data are expressed as means ± standard deviations (SD). Data with several groups were compared using one-way analysis of variance followed by Tukey's test, whereas student's t-test was used to compare two groups, using the GraphPad Prism 8 (GraphPad Software, Inc.; Dotmatics) software. One-way ANOVA followed by Tukey's post-hoc test was used to compare multiple treatment groups. P<0.05 was considered to indicate a statistically significant difference. All experiments were repeated three times. Statistical significance was set at *P<0.05, **P<0.01 and ***P<0.001.

Results

Screening of DEGs. The high-throughput sequencing datasets of GSE121212 and GSE157194 was obtained from GEO and analyzed using the R-packages limma (version 3.40.6) to target DEGs based on a criteria of log-fold change >2 and P<0.05. A total of 1,547 DEGs were identified in the GSE121212 dataset, with 920 genes found to be upregulated and 627 downregulated. A total of 1,031 DEGs were identified in the GSE157194
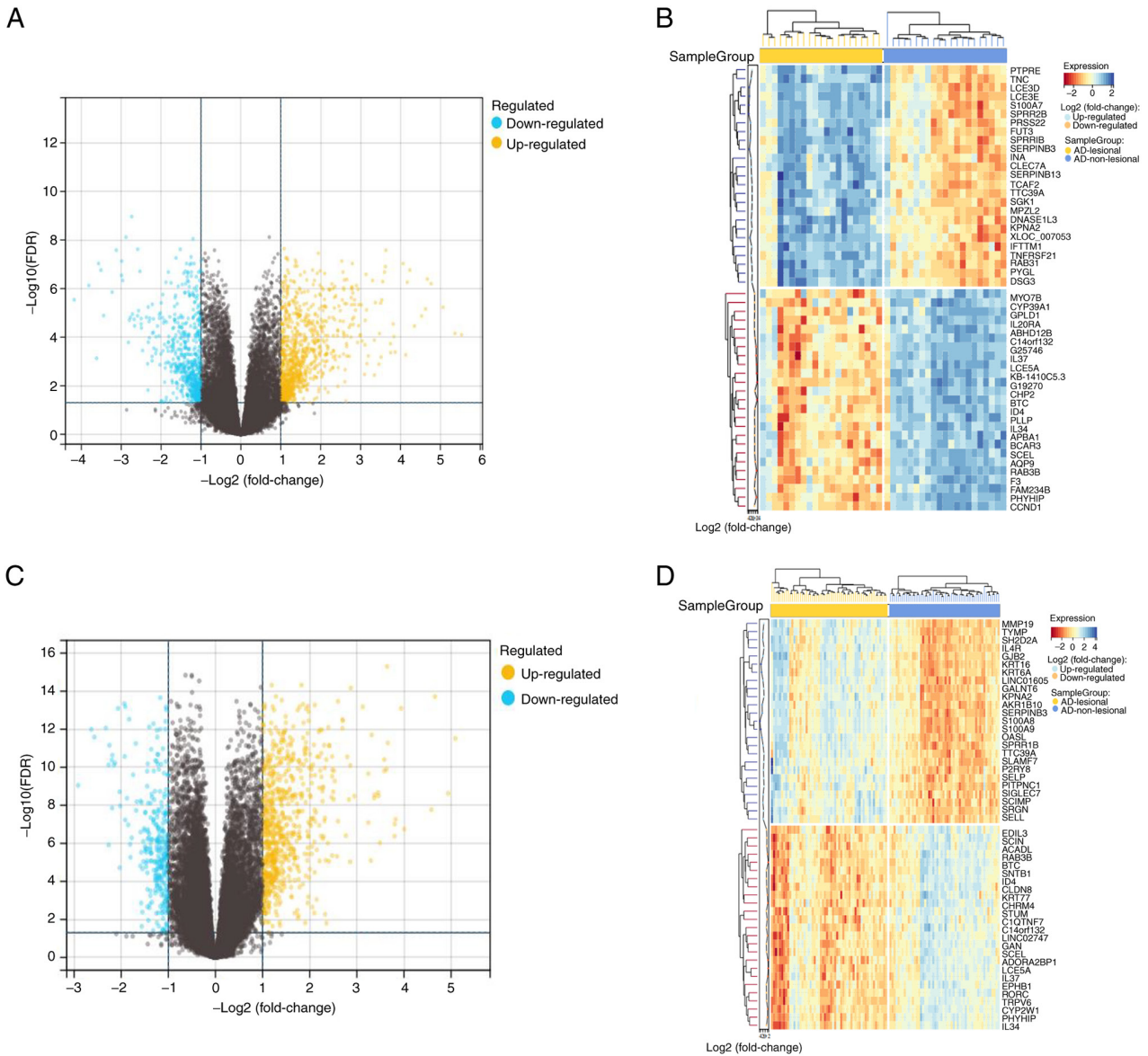
A

B

C

D

Figure 1. Volcano and heat maps of differentially expressed genes in the GSE121212 and GSE157194 datasets. (A) Volcano plot of differentially expressed genes in GSE121212. (B) Heat map of differentially expressed genes in GSE121212. (C) Volcano plot of differentially expressed genes in GSE157194. (D) Heat map of differentially expressed genes in GSE157194.

dataset, with 731 genes being upregulated and 300 downregulated. The results were visualized by generating volcano and heat maps of the DEGs (Fig. 1).

Screening for differentially co-expressed genes in the two datasets. The online bioinformatics analysis tool VENNY was used to screen for the differentially co-expressed genes. A total of 519 co-expressed differential genes were screened out (Fig. 2).

Analysis of functional GO and KEGG pathway-enriched co-expressed differential genes. The 519 differentially co-expressed genes were then underwent functional GO accumulation analysis and KEGG pathway accumulation analysis. In total 1,023 functions were subjected to GO analysis, with annotations categorized into BP, CC and MF. For BP, the co-expressed differential genes were found significantly enriched in the 'process of the immune
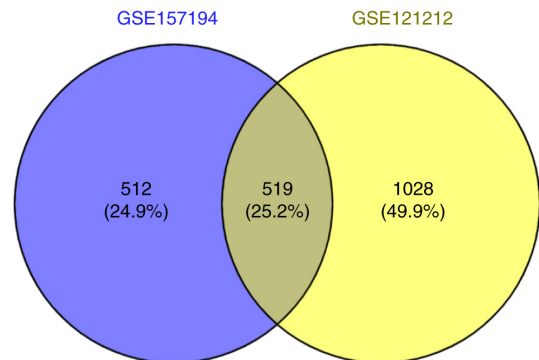

Figure 2. Differentially co-expressed genes between the GSE121212 and GSE157194 datasets.

system' and 'immune response.' In terms of CC and MF, the co-expressed differential genes were significantly enriched
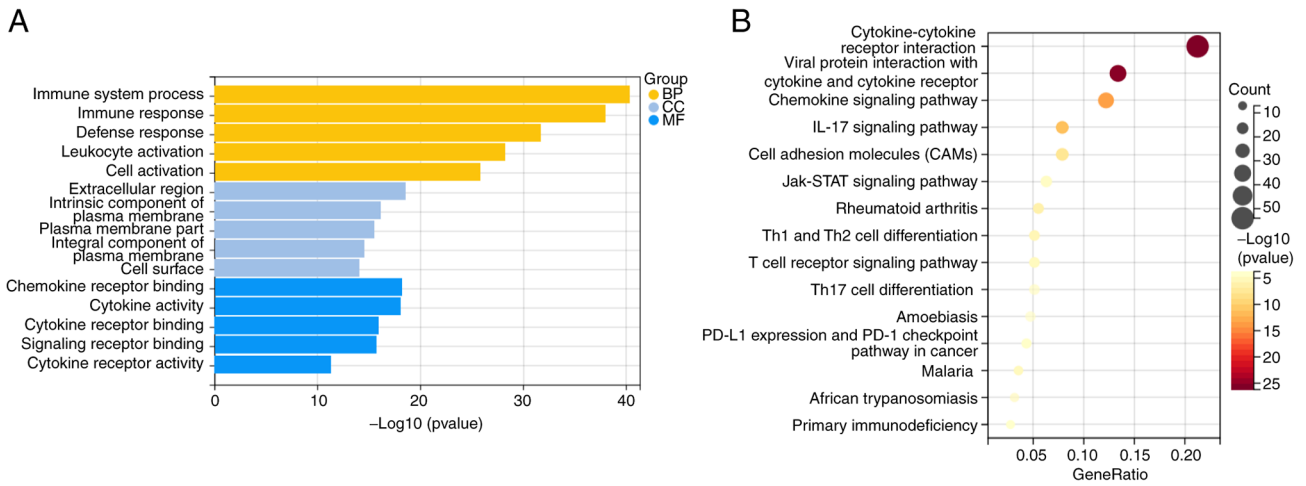
Figure 3. GO and KEGG enrichment analysis of co-expressed differentially expressed genes. (A) GO function enrichment analysis was performed on the selected differentially expressed genes enriched in three aspects: Biological process, cellular component, molecular function. (B) The 15 major signaling pathways were enriched by KEGG. GO, gene ontology; KEGG, Kyoto Encyclopedia of Genes and Genomes.
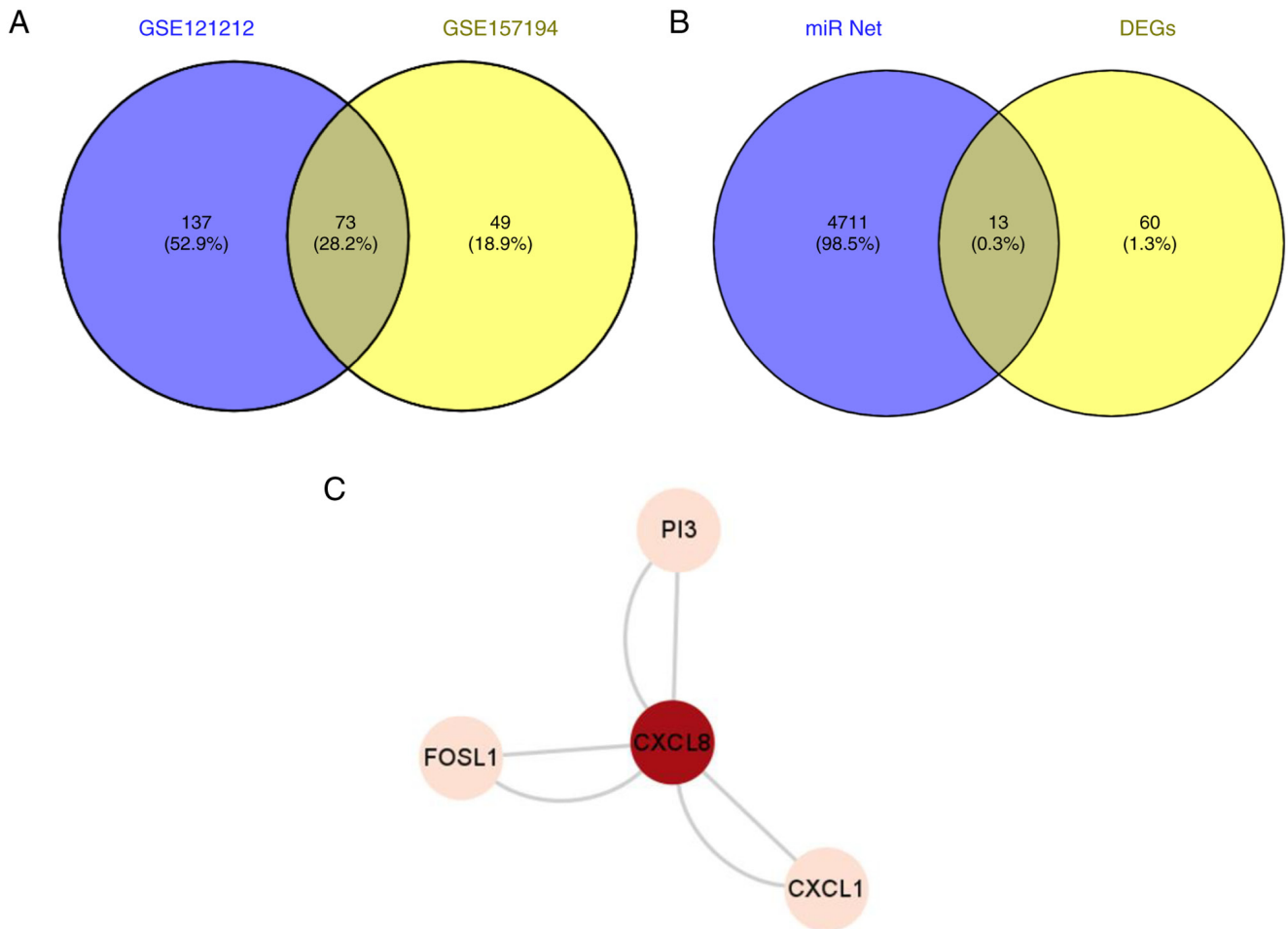

Figure 4. Prediction of target genes of miR-155-3p. (A) Selected 73 significantly differentially expressed genes from the GSE121212 and GSE157194 datasets. (B) The VENNY website was used to screen the intersection for significantly differentially expressed genes and the downstream target genes of miR-155-3p. A total of 13 genes were screened out. (C) Protein-protein interactions of PI3, FOSL1, CXCL1 and CXCL8 were generated using STRING database. miR, microRNA; CXCL, C-X-C motif chemokine ligand; FOSL1, FOS like 1; AP-1 transcription factor subunit; PI3, peptidase inhibitor 3.

in the 'extracellular region' and 'chemokine receptor binding', respectively (Fig. 3A). In addition, critical signaling pathways were identified using KEGG enrichment analysis. The co-expressed differential genes were found to be significantly enriched in the 'cytokine-cytokine receptor interaction' (Fig. 3B).

Prediction of target genes of miR-155-3p. The miRNet website was used to predict the downstream target genes of miR-155-3p. miRNet predicted 4,724 possible downstream targets. To assess the reliability of the results, the GSE121212 and GSE157194 datasets were screened on a smaller scale. The significant DEGs were identified using the criteria log-fold change >2 and P<0.05. A total of 210 significant DEGs were identified in the GSE121212 dataset, with 158 genes being upregulated and 52 downregulated. By contrast, 122 significant DEGs were screened from the GSE157194 dataset, of which 106 genes were upregulated and 16 genes were downregulated.

The significant DEGs of the two datasets were then cut using the online bioinformatics analysis tool VENNY 2.1.0, from which 73 significantly differentially co-expressed genes were obtained (Fig. 4A). The miR-net-predicted intersection of 73 significant DEGs and possible miR-155-3p downstream target genes was then obtained from the VENNY 2.1.0 site, yielding 13 genes (Fig. 4B). These genes included CXCL8, keratin 6B, selectin E, PI3, glutathione-Specific γ-glutamylcyclotransferase 1, transcobalamin 1, 2'-5'-oligoadenylate synthetase-like, CXCL1, C6orf223, insulin growth factor-like family member 1, MMP1, aldo-keto reductase family 1 member B10 and FOSL1.

Using The Human Protein Atlas website, the transcript levels of these 13 proteins in HaCaT cells were searched (Table I). The results showed that among the 13 proteins, PI3, FOSL1, CXCL8 and CXCL1 were the four proteins with the highest expression levels in HaCaT cells, where possible interaction among these four proteins was predicted (Fig. 4C).

Through functional GO accumulation analysis and KEGG pathway accumulation analysis, chemokines appeared to serve a particularly important role in the skin immune microenvironment in the setting of AD. Therefore, it was speculated that PI3, FOSL1, CXCL8 and CXCL1 can serve an important role in the epidermal immune microenvironment of patients with AD. The effects of miR-155 on PI3, FOSL1, CXCL8 and CXCL1 were therefore next focused upon for subsequent *in vitro* cell experiments.

miR-155 can inhibit the proliferation of HaCaT cells and promote the secretion of pro-inflammatory cytokines. To study the role of miR-155 in human keratinocytes (HaCaT cells), miR-155 mimics, mimics NC, miR-155 inhibitor and inhibitor NC we transfected with Lipofectamine® 2000 (Thermo Fisher Scientific, Inc.) transient transfection. After transfection of miR-155 mimics, mimics NC, miR-155 inhibitor and inhibitor NC in HaCaT cells for 24 h, the molecular level of miR-155 in HaCaT cells was detected by RT-qPCR. The transfection efficiency of miR-155 was detected. Compared with the mimics NC group and the control group, the relative expression of miR-155 was significantly increased in the miR-155 mimics group (P<0.001). There was no significant difference in the relative expression of miR-155 between mimics NC group, inhibitor NC group and control group. There was no significant difference in the relative expression of miR-155 between the miR-155 inhibitor group and the inhibitor NC group (Fig. 5A). As miR inhibitor can competitively bind to the downstream target genes of mature miR and weaken the silencing effect of miR. Generally, miRs are not degraded, so the molecular level of miR-155 can be detected by RT-qPCR. This result

Table I. RNA expression data of genes in HaCaT cells.

Gene	Normalized TPM value
CXCL8	48.2
CXCL1	38.6
FOS-like 1, AP-1 transcription factor subunit	60.6
Peptidase Inhibitor 3	109.8
Keratin 6B	3.9
Selectin E	0
Glutathione-Specific γ-glutamylcyclotransferase 1	6.0
Transcobalamin 1	5.5
2'-5'-Oligoadenylate synthetase-like	6.4
C6orf223	0
Insulin growth factor-like family member 1	6.9
MMP1	4.6
Aldo-keto reductase family 1 member B10	6.2

TPM, transcript per million; CXCL, C-X-C motif chemokine ligand.

suggested that transfection of miR-155 mimics in HaCaT cells can significantly increase the expression level of miR-155, which can be used for subsequent experimental studies.

HaCaT cells were seeded into 96-well plates at a density of 1.5×10^4 cells/well. Cell Count Kit-8 (CCK8) reagent was then added at 90% cell confluency. After 2 h incubation, the absorbance value of each well was measured at a wavelength of 450 nm using a microplate reader. Compared with the NC group, proliferation of HaCaT cells transfected with miR-155 mimics was found to be significantly inhibited (P<0.001; Fig. 5B). This result suggested that miR-155 can inhibit the proliferation of HaCaT cells.

Cytokines serve an important role in the pathogenesis of AD. According to the aforementioned GO and KEGG analyses, cytokines likely serve an important role in the epidermal immune microenvironment of patients with AD. The potential effects of miR-155 on cytokine secretion by HaCaT cells were therefore next examined. Compared with those in the mimics NC group, the levels of IL-1β (P<0.001), IL-6 (P<0.001) and IL-15 (P<0.01) in the supernatant of HaCaT cells were found to be significantly increased in the miR-155 mimics group, whilst those of IL-10 were significantly decreased (P<0.001; Fig. 5C-F). These results suggest that the overexpression of miR-155 in HaCaT cells can induce the secretion of proinflammatory cytokines IL-1β, IL-6 and IL-15, whilst inhibiting the secretion of the anti-inflammatory factor IL-10.

Effects of miR-155 on the predicted target genes. From the aforementioned experiments, high expression of miR-155 can inhibit the proliferation of HaCaT cells while promoting the secretion of pro-inflammatory cytokines. Through bioinformatic analysis, several potential miR-155 target genes were screened out, including PI3, FOSL1, CXCL1 and CXCL8. To determine the effects of miR-155 on the expression of
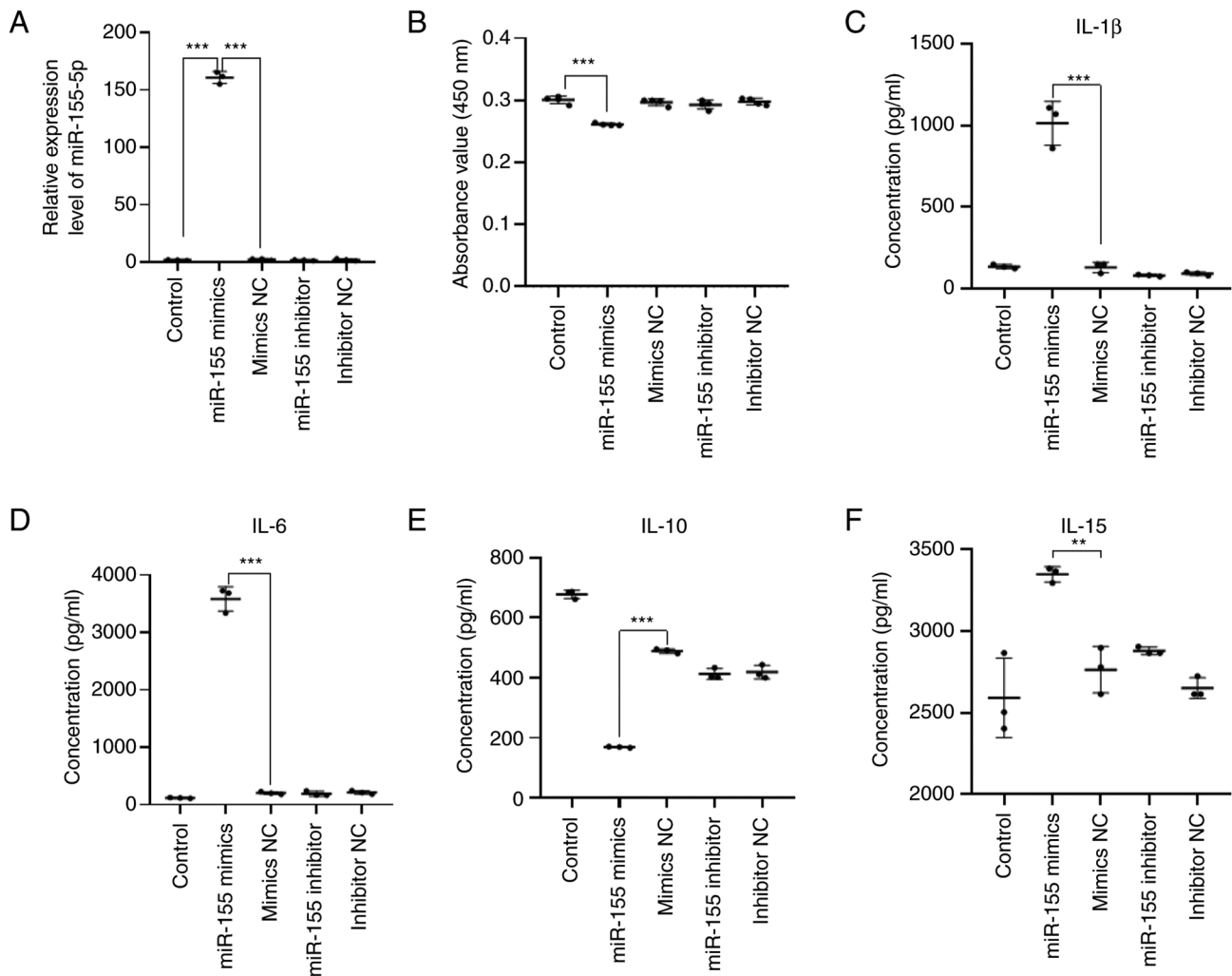
Figure 5. Effects of miR-155 on proliferation and cytokine secretion by HaCaT cells. (A) Transfection of miR-155 mimics in HaCaT cells can significantly increase the expression level of miR-155. (B) Overexpression of miR-155 in HaCaT cells can significantly inhibit HaCaT cell proliferation. Secretion of (C) IL-1β, (D) IL-6, (E) IL-10 and (F) IL-15 were detected by ELISA. **P<0.01, ***P<0.001. miR, microRNA.

these potential target genes and mechanism, changes in the expression of PI3, FOSL1, CXCL1 and CXCL8, in addition to the levels of CXCL1 and CXCL8 secretion into the culture supernatant of HaCaT cells, were measured by RT-qPCR and ELISA following miR-155 overexpression. RT-qPCR results revealed that compared with those in the mimics NC group, the expression levels of PI3 (P<0.001) and CXCL8 (P<0.001) were significantly reduced in the miR-155 mimics group, whereas those of FOSL1 (P<0.001) were increased. However, there was no significant difference in the expression of CXCL1 in the miR-155 mimics group (Fig. 6A-D). ELISA found that the level of CXCL1 secretion (P<0.001) was significantly increased in the miR-155 mimics group compared with that in the mimics NC group, whilst the secretion level of CXCL8 (P<0.001) was significantly decreased (Fig. 6E and F). These results suggested that miR-155 overexpression in HaCaT cells under physiological conditions resulted in decreased PI3 expression, increased FOSL1 and CXCL1 secretion, but decreased CXCL8 expression and secretion.

Effects of TNF-α and IFN-γ treatment on HaCaT cell prolifera-tion and cytokine secretion. To examine the effect of TNF-α and

IFN-γ on the expression of miR-155 in HaCaT cells, 5 ng/ml TNF-α and IFN-γ were added into the HaCaT cell culture medium for 6 h, before the medium was changed and further incubation for 48 h. The expression level of miR-155 in the cells was then detected by RT-qPCR. Compared with that in the control group, the expression level of miR-155 was significantly increased after TNF-α and IFN-γ stimulation (P<0.01; Fig. 7A). These results suggested that stimulation of HaCaT cells with TNF-α and IFN-γ increased miR-155 expression levels in HaCaT cells.

The HaCaT cells treated with TNF-α and IFN-γ and transfected were then divided into the following three groups: Control group; TNF-α + IFN-γ group; and TNF-α + IFN-γ + miR-155 overexpression group.

Following the aforementioned treatments, the cells were seeded into 96-well plates at a density of 1.5x10⁴ cells/well, before proliferation of each group was detected by CCK8 assay. The results showed that cell proliferation was significantly increased in the TNF-α + IFN-γ group (P<0.01) compared to the control group, whereas that in the TNF-α + IFN-γ + miR-155 overexpression group (P<0.001) was significantly inhibited compared with that in the control group. Compared with that in the TNF-α + IFN-γ group, cell proliferation was
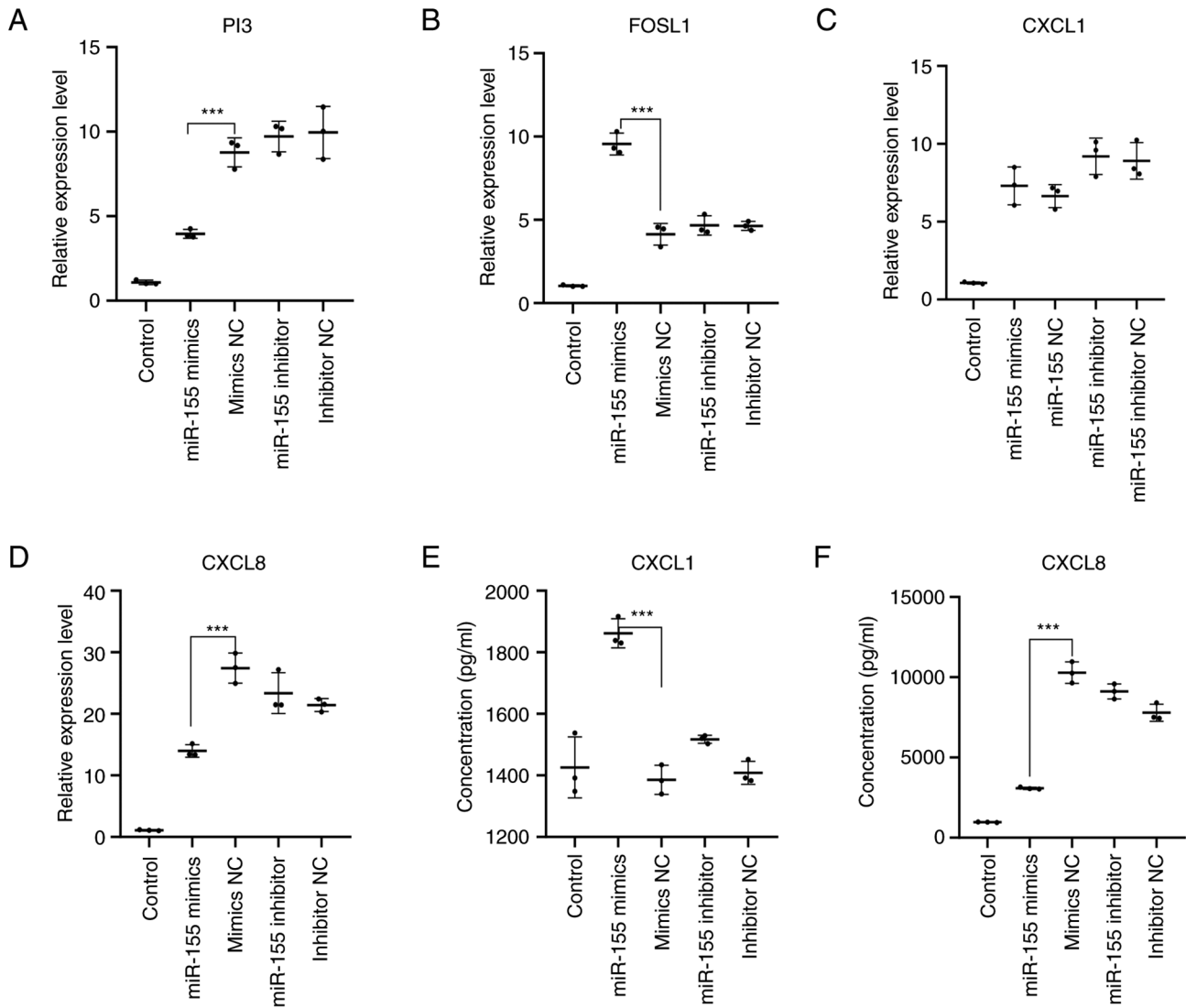
Figure 6. Effect of miR-155 on predicted target genes. mRNA expression level of (A) PI3, (B) FOSL1, (C) CXCL1, (D) CXCL8 was detected by reverse transcription-quantitative PCR. (E) CXCL1 and (F) CXCL8 levels in the culture medium of HaCaT cells was measured by ELISA. ***P<0.001. miR, microRNA; CXCL, C-X-C motif chemokine ligand; FOSL1, FOS like 1; AP-1 transcription factor subunit; PI3, peptidase inhibitor 3.

significantly inhibited in the TNF-α + IFN-γ + miR-155 overexpression group (P<0.001; Fig. 7B). These results suggest that miR-155 can inhibit the proliferation of HaCaT cells under the TNF-α- and IFN-γ-induced inflammatory state.

The inflammatory cell model of HaCaT cells was established by stimulating HaCaT cells with TNF-α and IFN-γ. The supernatant of the cell culture medium in the three groups was then collected before the level of IL-1β, IL-6, IL-10 and IL-15 were detected using ELISA. Compared with that in the control group, the secretion of IL-1β (P<0.001), IL-6 (P<0.001), IL-10 (P<0.001) and IL-15 (P<0.001) by HaCaT cells in the TNF-α + IFN-γ and the TNF-α + IFN-γ + miR-155 overexpression groups were significantly increased. Compared with that in the TNF-α + IFN-γ induction group, the secretion of IL-1β (P<0.05) and IL-6 (P<0.05) was increased in the TNF-α + IFN-γ + miR-155 overexpressed group, whilst the secretion of IL-10 and IL-15 did not change (Fig. 7C-F) These results suggested that miR-155 can promote the secretion of the proinflammatory cytokines IL-1β and IL-6 in HaCaT cells under the induction of TNF-α and IFN-γ.

Effect of miR-155 on TNF-α- and IFN-γ- induced target genes. The inflammatory cell model of HaCaT cells was constructed by stimulating HaCaT cells with TNF-α and IFN-γ. The expression levels of PI3, FOSL1, CXCL1 and CXCL8 were then detected by RT-qPCR, whereas western blotting was used to measure the protein expression levels of PI3 and FOSL1. The levels of CXCL1 and CXCL8 in the supernatant of HaCaT cells were detected by ELISA.

Compared with those in the control group, the mRNA and protein expression levels of PI3 (P<0.05) and FOSL1 (P<0.01) whereas the mRNA expression levels and secretion of CXCL1 (P<0.001) and CXCL8 (P<0.001) were significantly increased in the TNF-α + IFN-γ group and the TNF-α + IFN-γ + miR-155 overexpression group.

Compared to the TNF-α + IFN-γ group, the expression of PI3 (P<0.001) and CXCL1 (P<0.01) were significantly increased in the TNF-α + IFN-γ + miR-155 overexpression group. In addition, there was a significant increase in the mRNA expression level and secretion of CXCL8 (P<0.05) but no alterations could be detected in the expression of FOSL1 mRNA (Fig. 8).
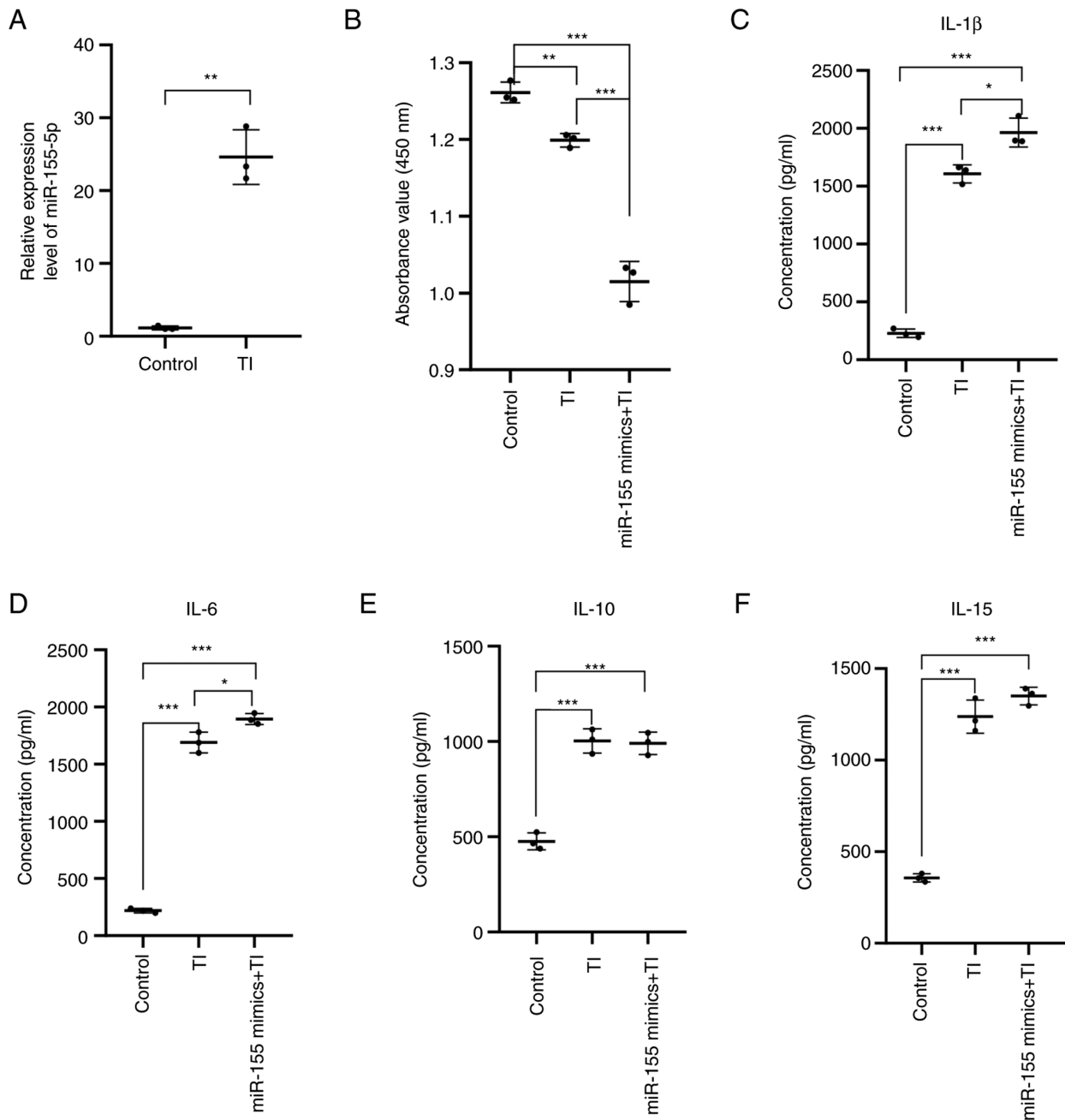
Figure 7. Effects of TNF-α and IFN-γ on the proliferation and cytokine secretion by HaCaT cells. (A) The expression level of miR-155 in TNF-α- and IFN-γ-stimulated HaCaT cells was determined by reverse transcription-quantitative PCR. (B) Cell Counting Kit-8 assay was used to detect TNF-α- and IFN-γ-induced -cell proliferation. Levels of (C) IL-1β, (D) IL-6, (E) IL-10 and (F) IL-15 in the culture medium of HaCaT cells were measured by ELISA. *P<0.05, **P<0.01, ***P<0.001. miR, microRNA.

These results suggested that miR-155 overexpression can increase PI3 and FOSL1 protein expression and CXCL1 and CXCL8 secretion, specially PI3 protein expression and CXCL8 secretion under inflammatory conditions. This was mainly mediated by significantly increasing the expression of proinflammatory factors CXCL1 and CXCL8 and the anti-inflammatory factors PI3. It is involved in the inflammatory response.

Discussion

AD is a chronic inflammatory skin disease that can exert significant psychosocial effects on patients and their families. AD can also increase the risk of asthma, allergic rhinitis and food allergy. The pathogenesis of AD is complex and involves the interaction among genetics, skin barrier and the immune system. Destruction of the skin barrier function can lead to skin barrier dysfunction, alter the molecular immune profile and the function of immune cells in the epidermal microenvironment, which then trigger skin inflammation in patients with AD. This in turn results in immune system imbalance, which will further aggravate skin barrier dysfunction.

Keratinocytes are an important component of the skin. They act as a skin barrier and serve an immunomodulatory role (16). Activated keratinocytes can secrete a variety of cytokines and chemokines, such as IL-1, IL-6, thymic stromal lymphopoietin and TNF-α., which serve an
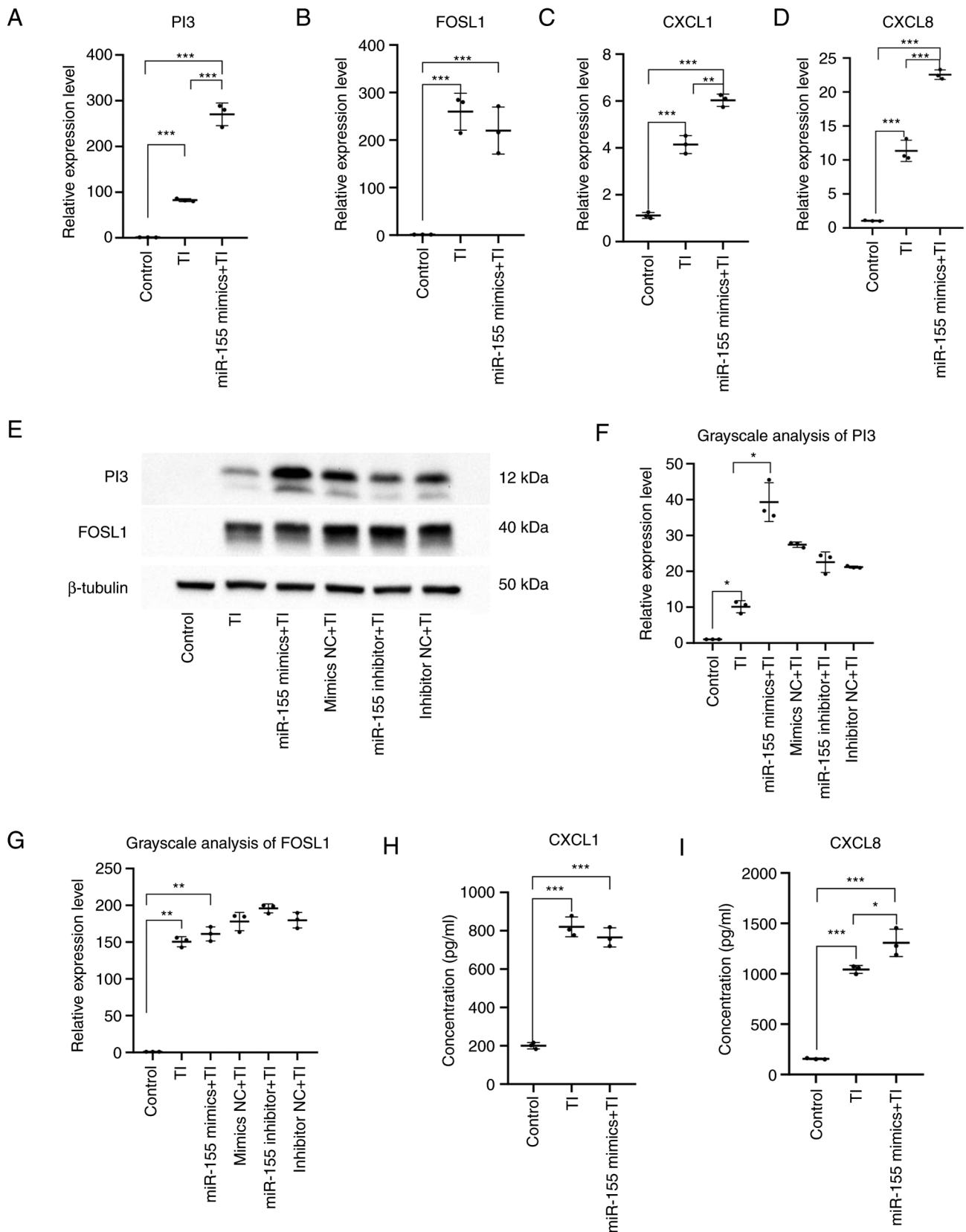
Figure 8. Effect of miR-155 on target genes induced by TNF-α and IFN-γ. mRNA expression of (A) PI3, (B) FOSL1, (C) CXCL1 and (D) CXCL8 was determined by reverse transcription-quantitative PCR. (E) Western blotting analysis of PI3 and FOSL1 protein concentrations. Semi-quantitative analysis of the Western blot Results detected for (F) PI3 and (G) FOSL1. (H) CXCL1 and (I) CXCL8 levels were detected by ELISA. *P<0.05, **P<0.01 and ***P<0.001. miR, microRNA; CXCL, C-X-C motif chemokine ligand; FOSL1, FOS like 1, AP-1 transcription factor subunit; PI3, peptidase inhibitor 3.

important role in the regulation of the epidermal immune microenvironment and skin barrier function (17). HaCaT

cells are widely used for *in vitro* studies of AD-associated skin conditions.

A number of studies have shown that miR-155 is involved in a variety of immune-related diseases by regulating inflammatory responses (18,19). In monocytes/macrophages, miR-155 has been reported to regulate inflammatory responses that are activated by certain cytokines (such as TNFα, IL-1β) or Toll-like receptor ligands in various cell types (18,20). In addition, miR-155 can promote M1 macrophage polarization, leading to local inflammation in the heart and even systemic inflammation in distant organs (21). miR-155 expression was found to be significantly increased in skin lesions of patients with AD (10). A previous study demonstrated that miR-155 can enhance IL-1 production by targeting SOCS17 (18). It has also been shown that miR-155 can coordinate with the NACHT domain-, leucine-rich repeat- and PYD-containing protein 3 inflammasome to drive IL-1β-mediated signaling, which further promotes IL-1β release and miR-155 expression (20). The increase in peripheral blood IL-6 levels in patients with AD is associated with the activation of T cells (22). IL-1β can mediate innate immune responses and skin inflammatory responses in various skin diseases, including psoriasis, vitiligo, systemic lupus erythematosus and AD (23,24). The present study revealed that elevated expression levels of miR-155 led to the release of the pro-inflammatory cytokines IL-1β, IL-6 and IL-15 whilst inhibiting the secretion of the anti-inflammatory cytokine IL-10. Although according to the present study miR-155 can promote the immune response in skin lesions of patients with AD, the underlying mechanism of action remain unconfirmed.

TNF-α and IFN-γ are cytokines that have been recognized to induce inflammation in HaCaT cells. To study the immune microenvironment in AD lesions, an inflammatory model of HaCaT cells was constructed. miR-155 has been shown to target and bind annexin A2 to regulate microvascular integrity and endothelial barrier function (25). The present study showed that the expression level of miR-155 was induced by TNF-α and IFN-γ in HaCaT cells and the expression level of miR-155 was increased after TNF-α and IFN-γ stimulation in HaCaT cells, whereas the high expression of miR-155 significantly inhibited the proliferation of HaCaT cells.

In the present study, four potential target genes of miR-155, PI3, FOSL1, CXCL1 and CXCL8, were identified by bioinformatic analysis. Through GO and KEGG accumulation analysis, it was found that chemokines and their signaling pathways probably serve an important role in AD lesions. Furthermore, PI3, FOSL1 and CXCL1 were each found to interact with CXCL8 following the construction of the protein interaction network of the four genes. The PI3 gene is a serine protease inhibitor that can inhibit excessive damage to elastase released by neutrophils during the inflammation process to resist the inflammatory response, antiviral and immunomodulatory effects (26-30). It has been previously reported that PI3 levels are increased in the blood of children with AD (31). However, the mechanism of PI3 in AD has not been studied. FOSL1 is a regulator of cell proliferation, differentiation, inflammation, tumorigenesis and metastasis and is involved in various proinflammatory responses (32-34). Although FOSL1 can induce inflammation, the mechanism of FOSL1 in AD remain unclear. CXCL1 and CXCL8 are important mediators of the inflammatory response and are involved in proinflammatory cascades mediating a number of inflammatory diseases (35-41). However, the specific roles and regulatory mechanisms of CXCL1 and CXCL8 in AD remain to be fully elucidated. Results from the present study showed that when HaCaT cells were stimulated with TNF-α and IFN-γ, the expression of miR-155, FOSL1, CXCL1 and CXCL8 was increased whereas the expression of PI3 was also increased. miR-155 overexpression can induce inflammation. If inflammatory factors persist in the environment, then the anti-inflammatory effect caused by the increased anti-inflammatory proteins will weaken. If miR-155 expression is increased, it can then induce immune cell infiltration into the immune microenvironment, where they can secrete a number of cytokines, such as IL-1, IL-6 and IL-15, whilst reducing the secretion of IL-10 and other anti-inflammatory cytokines, resulting in cytokine storm. Imbalance of inflammation regulation mechanism and increases in the inflammatory response can cause tissue and keratinocyte damage. Eventually, the skin's protective function is destroyed, resulting in idiopathic dermatitis.

Although the present study has found that miR-155 can regulate the production of PI3, FOSL1, CXCL1 and CXCL8 by HaCaT cells when stimulated with TNF-α and IFN-γ, the specific regulatory pathway downstream of miR-155 remain unclear. In addition, the effects of miR-155 on the level of immune molecules, the number and function of immune cells in the epidermal immune microenvironment of patients with AD require further study.

Availability of data and materials

The datasets used and/or analyzed during the current study are available from the corresponding author on reasonable request.

Authors' contributions

WQ and KG conceived and designed the study. XW, LC and CL conducted the data search. XW and XC performed the statistical and experiments analysis. XW and WQ drafted the manuscript. WQ and KG reviewed and edited the manuscript. XW and WQ confirm the authenticity of all the raw data. All authors read and approved the final manuscript.

Ethics approval and consent to participate

Not applicable.

Patient consent for publication

Not applicable.

Competing interests

The authors declare that they have no competing interests.

References

1. Silverberg JI and Hanifin JM: Adult eczema prevalence and associations with asthma and other health and demographic factors: A US population-based study. J Allergy Clin Immunol 132: 1132-1138, 2013.
2. Hay RJ, Johns NE, Williams HC, Bolliger IW, Dellavalle RP, Margolis DJ, Marks R, Naldi L, Weinstock MA, Wulf SK, *et al*: The global burden of skin disease in 2010: An analysis of the prevalence and impact of skin conditions. J Invest Dermatol 134: 1527-1534, 2014.
3. Patrick GJ, Archer NK and Miller LS: Which way do we go? Complex interactions in atopic dermatitis pathogenesis. J Invest Dermatol 141: 274-284, 2021.
4. Langan SM, Irvine AD and Weidinger S: Atopic dermatitis. Lancet 396: 345-360, 2020.
5. De Benedetto A, Kubo A and Beck LA: Skin barrier disruption: A requirement for allergen sensitization? J Invest Dermatol 132: 949-963, 2012.
6. Bangert C, Rindler K, Krausgruber T, Alkon N, Thaler FM, Kurz H, Ayub T, Demirtas D, Fortelny N, Vorstandlechner V, *et al*: Persistence of mature dendritic cells, T(H)2A and Tc2 cells characterize clinically resolved atopic dermatitis under IL-4Rα blockade. Sci Immunol 6: eabe2749, 2021.
7. Wongvibulsin S, Sutaria N, Kannan S, Alphonse MP, Belzberg M, Williams KA, Brown ID, Choi J, Roh YS, Pritchard T, *et al*: Transcriptomic analysis of atopic dermatitis in African Americans is characterized by Th2/Th17-centered cutaneous immune activation. Sci Rep 11: 11175, 2021.
8. Gross N, Kropp J and Khatib H: MicroRNA signaling in embryo development. Biology (Basel) 6: 34, 2017.
9. Chang J, Zhou B, Wei Z and Luo Y: IL-32 promotes the occurrence of atopic dermatitis by activating the JAK1/microRNA-155 axis. J Transl Med 20: 207, 2022.
10. Wang X, Chen Y, Yuan W, Yao L, Wang S, Jia Z, Wu P, Li L, Wei P, Wang X and Hong M: MicroRNA-155-5p is a key regulator of allergic inflammation, modulating the epithelial barrier by targeting PKIα. Cell Death Dis 10: 884, 2019.
11. Sonkoly E, Janson P, Majuri ML, Savinko T, Fyhrquist N, Eidsmo L, Xu N, Meisgen F, Wei T, Bradley M, *et al*: MiR-155 is overexpressed in patients with atopic dermatitis and modulates T-cell proliferative responses by targeting cytotoxic T lymphocyte-associated antigen 4. J Allergy Clin Immunol 126: 581-589, 2010.
12. Tsoi LC, Rodriguez E, Degenhardt F, Baurecht H, Wehkamp U, Volks N, Szymczak S, Swindell WR, Sarkar MK, Raja K, *et al*: Atopic dermatitis is an IL-13-dominant disease with greater molecular heterogeneity compared to psoriasis. J Invest Dermatol 139: 1480-1489, 2019.
13. Möbus L, Rodriguez E, Harder I, Stölzl D, Boraczynski N, Gerdes S, Kleinheinz A, Abraham S, Heratizadeh A, Handrick C, *et al*: Atopic dermatitis displays stable and dynamic skin transcriptome signatures. J Allergy Clin Immunol 147: 213-223, 2021.
14. Ritchie ME, Phipson B, Wu D, Hu Y, Law CW, Shi W and Smyth GK: limma powers differential expression analyses for RNA-sequencing and microarray studies. Nucleic Acids Res 43: e47, 2015.
15. Livak KJ and Schmittgen TD: Analysis of relative gene expression data using real-time quantitative PCR and the 2(-Delta Delta C(T)) method. Methods 25: 402-408, 2001.
16. Huang LY, Li ST, Lin SC, Kao CH, Hong CH, Lee CH and Yang LT: Gasdermin a is required for epidermal cornification during skin barrier regeneration and in an atopic dermatitis-like model. J Invest Dermatol 143: 1735-1745, 2023.
17. Jiang Y, Tsoi LC, Billi AC, Ward NL, Harms PW, Zeng C, Maverakis E, Kahlenberg JM and Gudjonsson JE: Cytokinocytes: The diverse contribution of keratinocytes to immune responses in skin. JCI Insight 5: e142067, 2020.
18. Testa U, Pelosi E, Castelli G and Labbaye C: miR-146 and miR-155: Two key modulators of immune response and tumor development. Noncoding RNA 3: 22, 2017.
19. Jankauskas SS, Gambardella J, Sardu C, Lombardi A and Santulli G: Functional role of miR-155 in the pathogenesis of diabetes mellitus and its complications. Noncoding RNA 7: 39, 2021.
20. Eissa MG and Artlett CM: The microRNA miR-155 is essential in fibrosis. Noncoding RNA 5: 23, 2019.
21. Hu C, Liao J, Huang R, Su Q and He L: MicroRNA-155-5p in serum derived-exosomes promotes ischaemia-reperfusion injury by reducing CypD ubiquitination by NEDD4. ESC Heart Fail 10: 1144-1157, 2023.
22. Toshitani A, Ansel JC, Chan SC, Li SH and Hanifin JM: Increased interleukin 6 production by T cells derived from patients with atopic dermatitis. J Invest Dermatol 100: 299-304, 1993.
23. Tang L and Zhou F: Inflammasomes in common immune-related skin diseases. Front Immunol 11: 882, 2020.
24. Bernard M, Carrasco C, Laoubi L, Guiraud B, Rozières A, Goujon C, Duplan H, Bessou-Touya S, Nicolas JF, Vocanson M and Galliano MF: IL-1β induces thymic stromal lymphopoietin and an atopic dermatitis-like phenotype in reconstructed healthy human epidermis. J Pathol 242: 234-245, 2017.
25. Barker KR, Lu Z, Kim H, Zheng Y, Chen J, Conroy AL, Hawkes M, Cheng HS, Njock MS, Fish JE, *et al*: MiR-155 modifies inflammation, endothelial activation and blood-brain barrier dysfunction in cerebral malaria. Mol Med 23: 24-33, 2017.
26. Ollague JE and Nousari CH: Expression of elafin in dermatitis herpetiformis. Am J Dermatopathol 40: 1-6, 2018.
27. Moreau T, Baranger K, Dade S, Dallet-Choisy S, Guyot N and Zani ML: Multifaceted roles of human elafin and secretory leukocyte proteinase inhibitor (SLPI), two serine protease inhibitors of the chelonianin family. Biochimie 90: 284-295, 2008.
28. Teng G, Liu Z, Liu Y, Wu T, Dai Y, Wang H and Wang W: Probiotic escherichia coli nissle 1917 expressing elafin protects against inflammation and restores the gut microbiota. Front Microbiol 13: 819336, 2022.
29. Li K, Zhang F, Wei L, Han Z, Liu X, Pan Y, Guo C and Han W: Recombinant human elafin ameliorates chronic hyperoxia-induced lung injury by inhibiting nuclear factor-kappa B signaling in neonatal mice. J Interferon Cytokine Res 40: 320-330, 2020.
30. Elgharib I, Khashaba SA, Elsaid HH and Sharaf MM: Serum elafin as a potential inflammatory marker in psoriasis. Int J Dermatol 58: 205-209, 2019.
31. Brunner PM, He H, Pavel AB, Czarnowicki T, Lefferdink R, Erickson T, Canter T, Puar N, Rangel SM, Malik K, *et al*: The blood proteomic signature of early-onset pediatric atopic dermatitis shows systemic inflammation and is distinct from adult long-standing disease. J Am Acad Dermatol 81: 510-519, 2019.
32. He YY, Zhou HF, Chen L, Wang YT, Xie WL, Xu ZZ, Xiong Y, Feng YQ, Liu GY, Li X, *et al*: The Fra-1: Novel role in regulating extensive immune cell states and affecting inflammatory diseases. Front Immunol 13: 954744, 2022.
33. Mishra RK, Potteti HR, Tamatam CR, Elangovan I and Reddy SP: c-Jun is required for nuclear factor-kappaB-dependent, LPS-stimulated fos-related antigen-1 transcription in alveolar macrophages. Am J Respir Cell Mol Biol 55: 667-674, 2016.
34. Moon YM, Lee SY, Kwok SK, Lee SH, Kim D, Kim WK, Her YM, Son HJ, Kim EK, Ryu JG, *et al*: The fos-related antigen 1-JUNB/Activator protein 1 transcription complex, a downstream target of signal transducer and activator of transcription 3, induces t helper 17 differentiation and promotes experimental autoimmune arthritis. Front Immunol 8: 1793, 2017.
35. Korbecki J, Barczak K, Gutowska I, Chlubek D and Baranowska-Bosiacka I: CXCL1: Gene, promoter, regulation of expression, mRNA stability, regulation of activity in the intercellular space. Int J Mol Sci 23: 792, 2022.
36. Korbecki J, Maruszewska A, Bosiacki M and Chlubek D and Baranowska-Bosiacka I: The potential importance of CXCL1 in the physiological state and in noncancer diseases of the cardiovascular system, respiratory system and skin. Int J Mol Sci 24: 205, 2022.
37. Zhu Y, Yang S, Zhao N, Liu C, Zhang F, Guo Y and Liu H: CXCL8 chemokine in ulcerative colitis. Biomed Pharmacother 138: 111427, 2021.

38. Kamsteeg M, Jansen PA, van Vlijmen-Willems IM, van Erp PE, Rodijk-Olthuis D, van der Valk PG, Feuth T, Zeeuwen PL and Schalkwijk J: Molecular diagnostics of psoriasis, atopic dermatitis, allergic contact dermatitis and irritant contact dermatitis. Br J Dermatol 162: 568-578, 2010.
39. Hulshof L, Hack DP, Hasnoe Q, Dontje B, Jakasa I, Riethmüller C, McLean WHI, van Aalderen WMC, Van't Land B, Kezic S, *et al*: A minimally invasive tool to study immune response and skin barrier in children with atopic dermatitis. Br J Dermatol 180: 621-630, 2019.
40. Liu Q, Li A, Tian Y, Wu JD, Liu Y, Li T, Chen Y, Han X and Wu K: The CXCL8-CXCR1/2 pathways in cancer. Cytokine Growth Factor Rev 31: 61-71, 2016.
41. DiStasi MR and Ley K: Opening the flood-gates: How neutrophil-endothelial interactions regulate permeability. Trends Immunol 30: 547-556, 2009.